Chapter 4

Nd:YAG Laser Welding for Photonics Devices Packaging

Ikhwan Naim Md Nawi, Jalil Ali, Mohamed Fadhali and Preecha P. Yupapin

Additional information is available at the end of the chapter

http://dx.doi.org/10.5772/50656

1. Introduction

The state-of-the art of the pulsed Nd:YAG laser spot welding for photonics device packaging has been introduced by Marley (Marley, 2002), which utilizes the laser for high precision joining and alignment. The advantages of laser welding over conventional fusion welding processes include precise welds with a high aspect ratio, narrow heat affected zone (HAZ), very little thermal distortion, ease of automation, high welding speed, enhanced design flexibility, clean, high energy density, low heat input and an efficient process (Zhou & Tsai, 2008; Kazemi & Goldak, 2009). One of the key features of laser welding is the ability to weld without filler materials and it offers distinct advantages (Pang et al., 2008). Laser welding is a liquid-phase fusion process. It joins metals by melting the interfaces and resulting the mixing of liquid molten metal. Then, it solidifies on the removal of the laser beam irradiation (Ready, 1997). Photonics devices used for telecommunications of military applications are usually required to operate for a long life of operation in fields with potentially humid, corrosive and mechanically turbulent environments. Therefore, long term reliability in such hostile operating conditions requires strong fixing of the aligned components and hermetic sealing of the photonics devices inside metal hybrid housings (Fadhali et al., 2007a). It is worth to mention that 60% to 80% of the photonics devices modules cost are due to the coupling and packaging processes. Therefore, understanding the effective packaging technique is very important to produce efficient and reliably packaged photonics devices. Moreover, care must be taken to assemble functional packages because only packages that can be manufactured reliably at competitive costs will survive in the business world. For photonics packaging applications, most of the welds are of butt or lap joints which require the weld penetration depth to be larger than the bead width. Moreover, for miniature packages that contain some sensitive coupling components, the penetration depth should be large enough to achieve a strong attachment (Fadhali et al.,

2007a, 2007b, 2007c, 2007d, 2008). At the same time, the bead width should be small to minimize the HAZ and hence prevent the damage to the sensitive optical components. The desired material for this application requires a low thermal conductivity or a higher electrical resistivity (Dawes, 1992). The lower the thermal conductivity of a material the more likely it is to absorb laser energy. For this reason, several weldable grades of steel and stainless steel are ideal for laser welding. The low carbon austenitic stainless steel (300 series steel) which has carbon level less than 0.1% produces good quality welds and reliable weld performance (Fadhali et al., 2007a; Naim et al., 2009). Hence, in this chapter, a stainless steel 304 is utilized as a base material for laser welding. It has been reported that other types of stainless steel were studied by other researchers. For instance, Mousavi and Sufizadeh investigated stainless steel 321 and 630 (Mousavi & Sufizadeh, 2008), while Beretta et al. studied stainless steel 420 (Beretta et al., 2007), for the application of pulsed Nd:YAG laser welding. Whilst a great deal of effort has been focused on developing processing systems there is an urgent need to understand the strength of the weldment. It is the aim of this chapter to examine the strength of a stainless steel 304 welded joint. Despite the pulsed Nd:YAG laser welding has been widely used in microelectronic and photonics packaging industry, a full understanding of various phenomena involved is still a matter of trials and speculations.

2. Mathematical model of penetration depth of a spot weld

Penetration depth of laser spot welding is one of the vital parameters that contributes to a good laser spot micro welding outcome. Practical penetration depth measurements are time consuming and laborious like cutting the samples in order to obtain the weld cross section. Thus, this section shows a theoretical model to estimate penetration depth inside the welded samples by controlling laser parameters or to predict the laser parameters at the required penetration depth. Figure 1 illustrates the penetration depth on a welding specimen. The 1-Dimensional model is developed base on the heat conduction and energy balance equations (Naim et al., 2010).

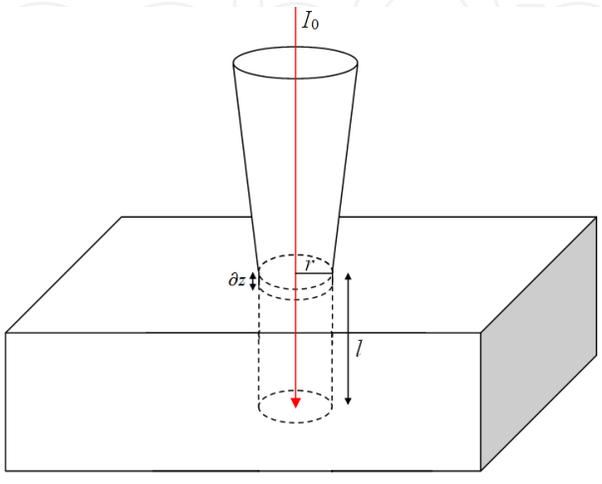

Figure 1. Illustration of the penetration depth of the focused laser beam on a welding specimen.

Applying the energy balance equation at the laser spot gives (Naim et al., 2010),

$$(1-R)I_0 = \rho L_m \frac{\partial l}{\partial t} - K\left(\frac{\partial T}{\partial z}\right)_{z=0} \tag{1}$$

Here I_0 is laser power density, L_m is latent heat of fusion, R is material reflectivity, ρ is material density, K is thermal conductivity, $\partial T / \partial z$ is temperature gradient at the welding front, l is the penetration depth, t is irradiation time and $\partial l / \partial t$ is penetration velocity. To determine the penetration velocity which is the change of penetration depth with time, the temperature gradient at the welding front should first be determined. The temperature distribution inside the target material is governed by the 1-Dimension heat conduction equation given as (Naim et al., 2010),

$$\frac{1}{\alpha}\frac{\partial T}{\partial t} = \frac{\partial^2 T}{\partial z^2} \tag{2}$$

where, α is thermal diffusivity. Equation (2) can be rewritten as

$$-\frac{1}{\alpha}\frac{\partial l_p}{\partial t}\frac{dT}{dz} = \frac{d^2 T}{dz^2} \tag{3}$$

The boundary conditions are taken as,

$$z=0,\ T=T_m \text{ and at } z\rightarrow\infty,\ T=T_0\ .$$

The maximum attainable temperature is the melting temperature of the material, T_m. Substituting these boundary conditions into Equation (3) and the solution for temperature distribution inside the material as

$$\frac{T-T_0}{T_m-T_0} = \exp\left[-\frac{1}{\alpha}\left(\frac{dl}{dt}\right)z\right] \tag{4}$$

The temperature gradient at the welding front can be obtained using Equation (4),

$$\left(\frac{dT}{dz}\right)_{z=0} = -\frac{1}{\alpha}\left(\frac{dl}{dt}\right)\left(T_m - T_0\right) \tag{5}$$

Substituting Equation (5) into the energy balance equation,

$$\left(1-R\right)I_0 = \rho L_m\left(\frac{dl}{dt}\right) + \rho c\frac{dl}{dt}\left(T_m - T_0\right) \tag{6}$$

From Equation (6), the welding velocity can be rewritten as,

$$\frac{dl}{dt} = \frac{\left(1-R\right)I_0}{\rho\left[L_m + c\left(T_m - T_0\right)\right]} \tag{7}$$

Integrating Equation (7) gives,

$$l = \frac{\left(1-R\right)Pt}{\pi r_o^2 \rho\left[L_m + c\left(T_m - T_0\right)\right]} \tag{8}$$

Here P is the laser peak power, t is the irradiation time or pulse duration and r is the laser beam radius. From Equation (8), one can observe that penetration depth is proportional to laser peak power and pulse duration as well as the material reflectivity.

Figure 2 illustrates the penetration depth versus peak power and pulse duration. Any changes of either peak power or pulse duration gives the same influence to the penetration depth. This is in agreement with the fact that the penetration depth increases linearly with both the peak powers and pulse durations. The penetration depth increases linearly with an increase of laser peak power. The higher laser peak power means more laser energy is absorbed into the welding material. When a higher laser energy is absorbed, it will produce a deeper melting pool. After solidification, the melting pool produces deeper weld or penetration depth. The trend is similar for variation of pulse duration. Higher pulse duration means longer heating duration. This will provide more time for laser beam to penetrate into the welding material. Thus, a deeper penetration depth will be produced. From Figure 3, it can be summarized that the penetration depth decreases significantly with laser spot radius. This is because the laser power density, I is proportional to $1/r^2$ and the power density will drop significantly as the laser spot radius increases. Laser power density determines the quantity of energy applied on welding material at a specific time. Higher power density will produce a deeper penetration depth.

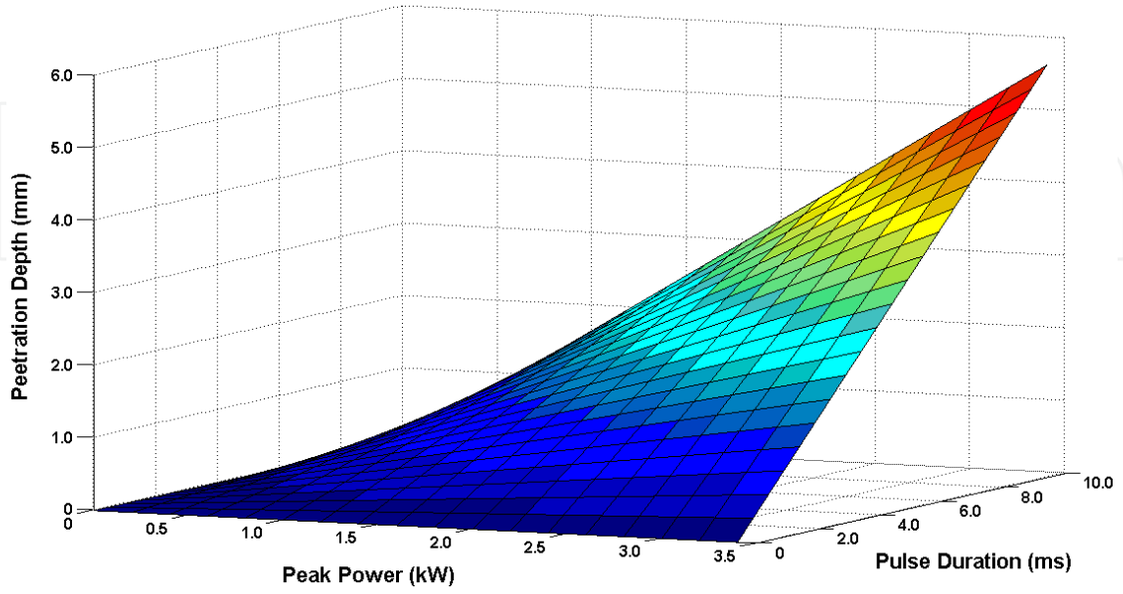

Figure 2. Penetration depth versus peak power and pulse duration.

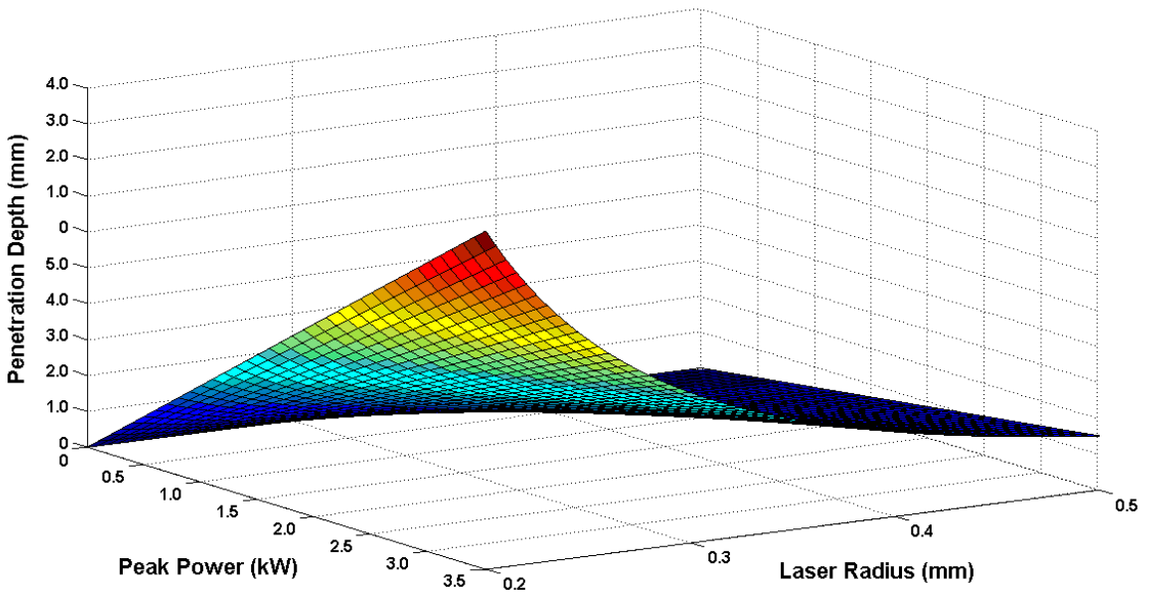

Figure 3. Penetration depth versus peak power and laser beam radius.

3. Mathematical model of laser beam power penetration

In order to produce a spot weld, a laser beam is incident on a specimen surface. The incident laser beam will be absorbed by the specimen depending on the material absorption coefficient. Thus, the absorbed laser beam heats up the specimen surface, raising its temperature. It will melt the specimen and produce a weld when it solidifies. The laser beam penetration in welding material has been derived using the continuity equation (Naim et al., 2010). It is assumed that laser beam penetrates the material based on a cylindrical coordinate. Figure 4 illustrates the laser beam power penetration in stainless steel specimen.

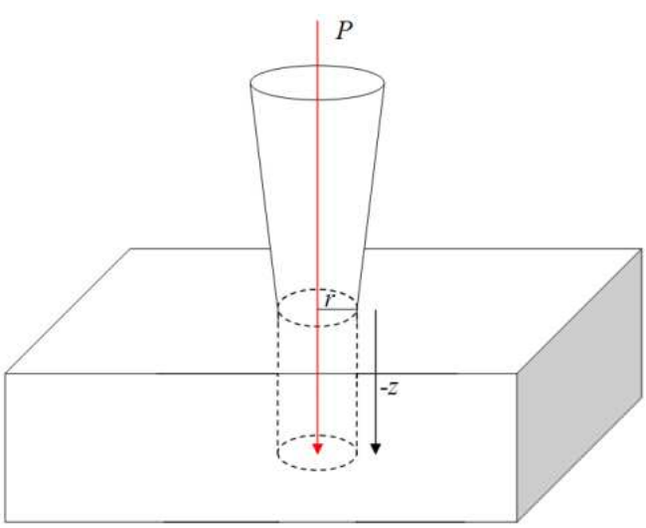

Figure 4. Laser beam power penetration in stainless steel specimen.

The laser beam power penetration is derived from a continuity equation given as (Naim, 2010),

$$\frac{\partial P}{\partial t} - k\nabla P = 0 \tag{9}$$

In cylindrical coordinate, Equation (9) then becomes,

$$\frac{\partial P}{\partial t} = k\left(\frac{\partial^2 P}{\partial r^2} + \frac{1}{r}\frac{\partial P}{\partial r} + \frac{\partial^2 P}{\partial z^2}\right) \tag{10}$$

Here $P=P(r,z,t)$ is the laser beam power penetration, r is the laser spot radius, z is the depth, k is the thermal conductivity and t is time. To solve this equation, let $P = RZT = R(r)Z(z)T(t)$ and the solutions are given by,

$$T = c_1 e^{-\mu^2 kt}, \tag{11}$$

$$R = c_2 J_0(\mu r) + c_3 Y_0(\mu r), \tag{12}$$

$$\text{and} \quad Z = c_4 e^{\mu z} + c_5 e^{-\mu z} \tag{13}$$

where c_1, c_2, c_3, c_4, c_5 and μ are the unknown constants and determined by the boundary conditions, J_0 is first order of Bessel function and Y_0 is second order of Bessel function. Equation (10) can be solved by using Equations (11), (12) and (13) giving,

$$P(r,z,t) = [c_1 e^{-\mu^2 kt}][c_2 J_0(\mu r) + c_3 Y_0(\mu r)][c_4 e^{\mu z} + c_5 e^{-\mu z}] \tag{14}$$

Let $A= c_1= c_2= c_3= c_4= c_5$ as the incident laser beam peak power and μ is the material absorption coefficient. In this calculation, only first order of Bessel function is considered. It is also assumed that the laser beam propagates only directing into the material which is $-z$ direction. Equation (14) can be written as,

$$P(r,z,t) = Ae^{-k\mu^2 t}[J_0(\mu r)][e^{-\mu z}] \tag{15}$$

For stainless steel material, the absorption coefficient, μ is 0.3 (Kazemi & Goldak, 2009) and the laser beam peak power used in this consideration is 3.5kW. Equation (15) then specified as,

$$P(r,z,t) = 3500e^{-0.3^2 kt}[J_0(0.3r)][e^{-0.3z}] \tag{16}$$

Equation (16) provides the time dependent laser beam penetration. The laser beam penetration is computed for its radius and depth. Figure 5 shows the profile of applied peak power versus the depth of specimen and laser spot radius. The peak power 3.500kW decreases exponentially with depth of stainless steel material and decreases according to the first order of Bessel function in terms of the spot radius. The peak power incident on the surface is 3.500kW at the centre of laser spot target, but decreases to 3.0248 kW at the spot radius of 0.25mm. Peak power reduces to 0.1743kW at the centre and 0.1506kW at spot radius of 0.25mm for a depth of 1.00mm. At the laser spot radius of 2.00mm, the laser beam is almost fully penetrated with only peak power of 0.0087kW at the centre of the penetration.

Figure 6 illustrates the time dependent laser beam penetration for stainless steel material. According to the illustration, the peak power reduces exponentially for both depth and time. From observation, laser beam peak power decreases faster through the depth rather than through the time, relatively. This is explained by Equation (16) which states penetrated laser beam is based on absorption coefficient through the depth is -0.03 m but only -0.0009 m through time. At a depth of 2.00 mm and time of 4.0 ms, the peak power is 0.0002 kW. At this point, laser beam is almost fully penetrated. On the interface between stainless steel material and laser beam spot, laser beam penetration can be illustrated by Figure 7 at certain time. As discussed before, laser beam penetration decreases according to the first order of Bessel function with the spot radius and exponentially with time. At the central of the interface, the peak power is 3.5 kW and it reduces to 0.0026 kW after 8.0 ms. At laser spot radius of 0.25 mm, the laser beam penetration is 3.0248 kW and it reduces to 0.0023 kW after 8.0 ms where the laser beam is about to fully absorbed by the stainless steel material.

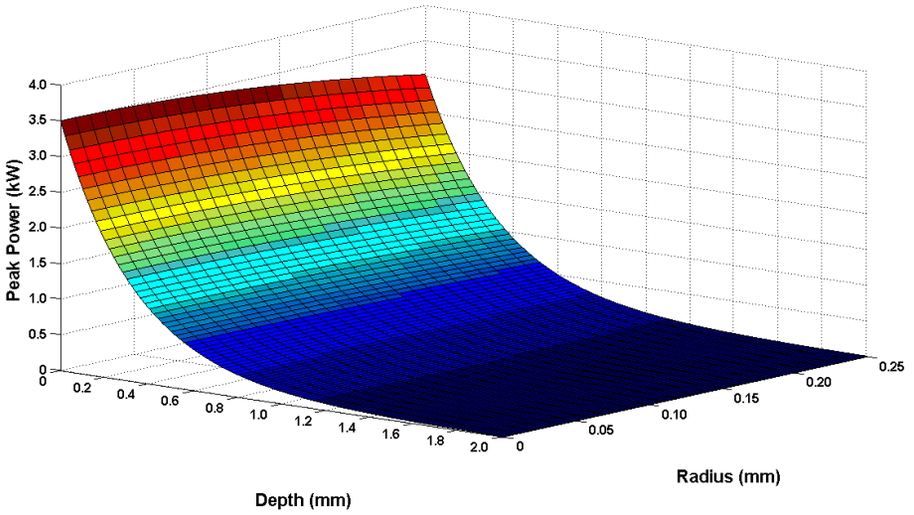

Figure 5. Peak power versus depth and radius for stainless steel with absorption coefficient, μ=0.3 and t=1 ms.

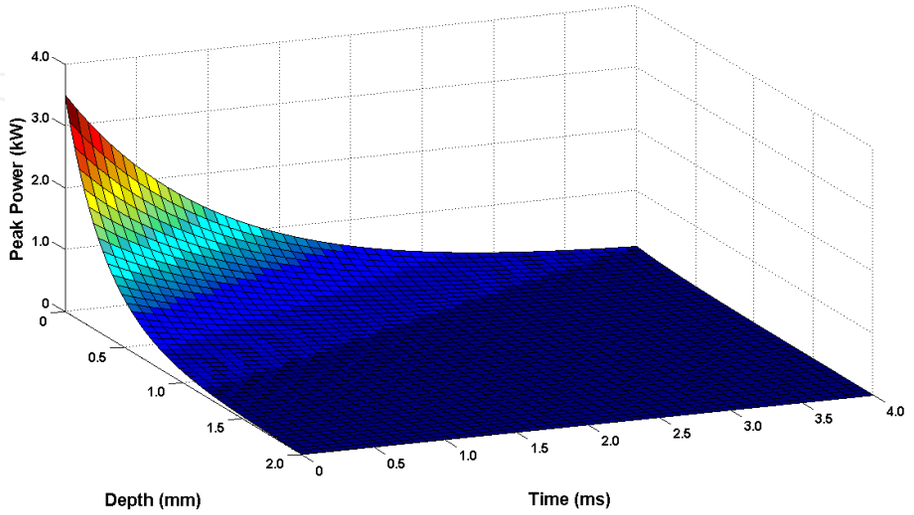

Figure 6. Peak power versus depth and time for stainless steel with absorption coefficient, μ=0.3 at the centre of penetration.

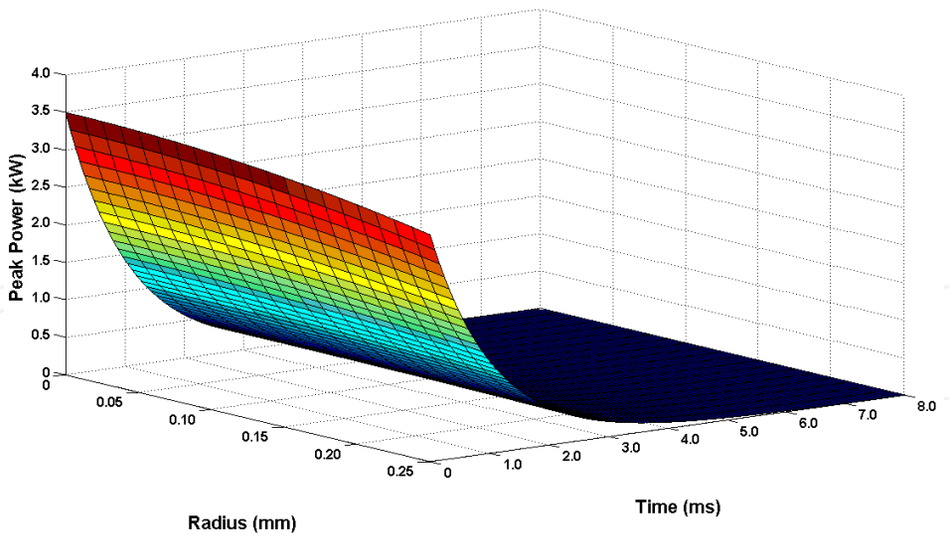

Figure 7. Peak power versus radius and time for stainless steel with absorption coefficient, μ=0.3 at the welding front.

4. Analysis of the pulsed Nd:YAG laser spot weld

The profiles for the penetration depth and bead width produced by the pulsed Nd:YAG laser beam are depicted in Figure 8 and Figure 9. The weld dimensions (weld penetration depth and bead width) for different laser beam peak powers are illustrated in Figure 10. The results display an increase in penetration depth and bead width with an increase in the laser beam peak power. The deepest penetration depth produced is 1.31 mm and the largest bead width is 0.57 mm when laser beam peak power is set at 3.5 kW. When laser beam peak power is reduced to 0.5 kW, the reading of penetration depth and the bead width are only 0.36 mm and 0.24 mm. The linear gradients of penetration depth and bead width are 0.301 and 0.10, respectively. These values show the laser beam peak power is almost 3 times more effective on the penetration depth rather than the bead width. This suggests that the laser beam peak power is a reliable parameter to control the desired penetration depth. It is observed in Figure 10 that the penetration depth and bead width increases when the pulse duration is increased. From the Figure 11, linear gradient of penetration depth and bead width are 0.0039 and 0.035, respectively. Only slight difference is noted and this means that the pulse duration has no significant effect either on penetration depth or bead width. As compared with the effect of laser peak power, the pulse duration is a much more better parameter to control the desired bead width.

Laser beam can be defocused by moving the focus point position forward or backward from the specimen surface. Figure 12 depicts that the penetration depth decreases significanly when the laser beam focus point position is moved from 0 to 4.0 mm with respect to the specimen surface. After 4.0 mm, the penetration depth decreases gradually untill 6.0 mm and there is no penetration depth that can be traced after 6.0 mm. Otherwise, when the focus point position is moved forward or backward, the bead width increases. But after 6.00 mm, there is no more bead width and only the sign of burning can be observed on the welding

surface. As the focus point position is moved forward or backward from the specimen surface, the laser spot size increases. This will reduce the intensity of the laser beam which is given by, $I_0=P/\pi r^2$. Here, P is the laser beam peak power and r is the laser spot radius. It indicates that the intensity of laser beam is negatively proportional with r^2. Hence, the laser beam does not have sufficient intensity to penetrate the material. As illustrated in Figure 13, it is observed that the penetration depth and bead width changes with the laser beam incident angle. As the laser beam incident angle increases, the laser spot becomes elliptical and wider. Hence the bead width also becomes elliptical and wider. The wider laser spot will reduce the intensity of the laser beam. This will result in a decrease of the penetration depth. However, when the laser beam incident angle is increased, the reflectivity of material surface drops due to the influence of light polarization. When the reflectivity drops, it will transport more laser energy into the welding material. Hence, it will increase the penetration depth. It can be seen that when weld penetration depth at angle of incidence of 45 degrees is much higher than that at 25 degrees. But, even though the reflectivity of the material surface drops greatly at 65 degrees, the penetration depth is only 0.82 mm because laser beam is less intense due to the significant increases in the laser spot area for a slight increase of the incident angle. In Figure 14, it can be seen that the penetration depth increases slightly with the number of shots. The penetration depth for the first and seventh pulse shots are 0.91 mm and 1.11 mm. When the first shot is applied it produces a shallow concave hole on the specimen surface. This is due to the material ablation produced by laser pulse pressure when it strikes the material surface. Then, when the second shot is given, it is able to go towards the bottom of the concave hole. The second shot weld penetration depth is similar to the first shot but with an increase in the depth of the concave hole. The first and seventh shot produce 0.52 mm and 0.57 mm of bead width. The difference is relatively small because the same laser beam parameters are used for each shot.

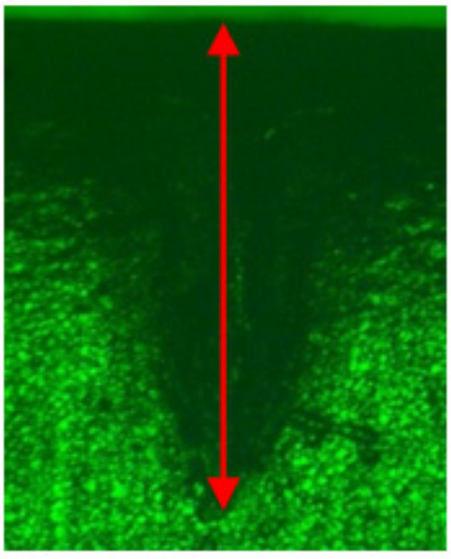

Figure 8. Cross-section of a spot weld produced by 2.5kW laser beam peak power and 2.5ms pulse duration. The penetration depth is labelled by the vertical line.

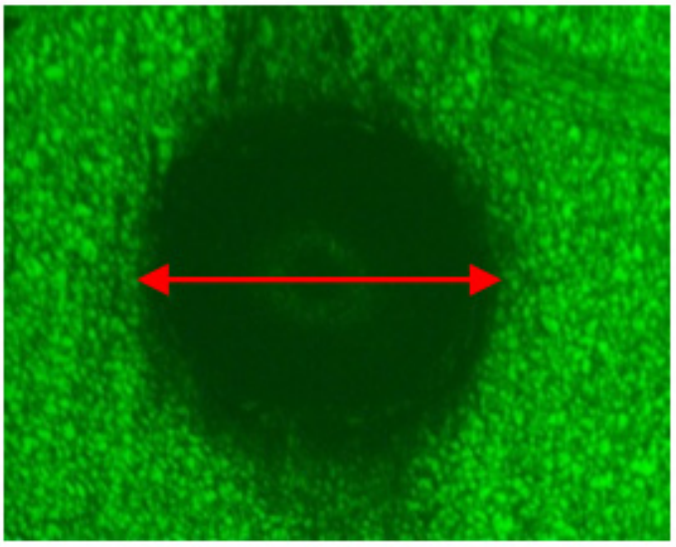

Figure 9. Figure 9. Top view of a spot weld produced by 2.5kW laser peak power and 2.5ms pulse duration. The bead width is labelled by the horizontal line.

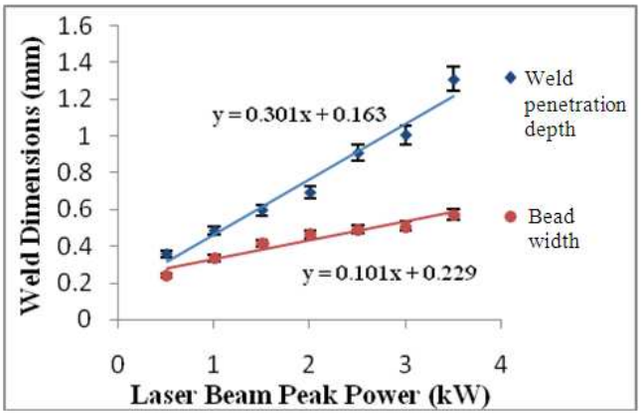

Figure 10. Characteristics of a spot weld dimensions as a function of laser peak powers conducted by 2.5 ms pulse duration with laser beam incidence is vertical in respect to the surface normal.

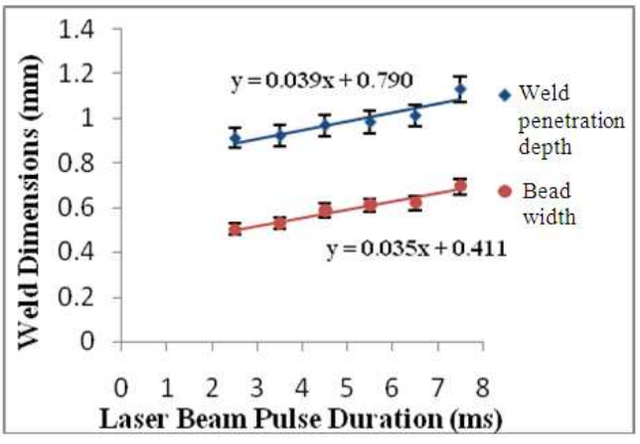

Figure 11. Characteristics of a spot weld dimensions as a function of laser pulse durations conducted by 2.5 kW laser peak power with wavelength of 1064 nm.

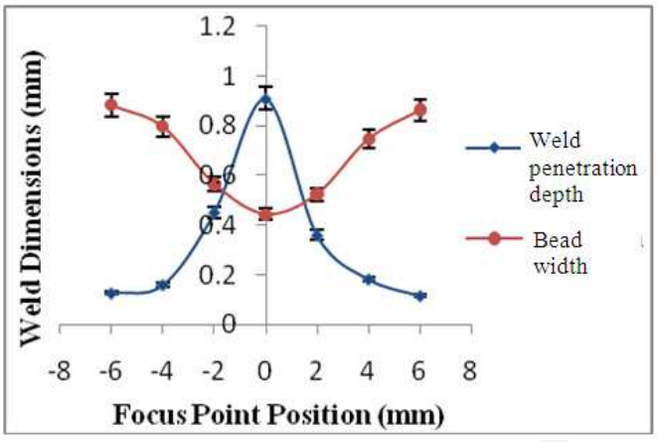

Figure 12. Characterictics of a spot weld dimensions when Nd:YAG laser spot is positioned forward and backward from the stainless steel 304 surface with 2.5 kW laser peak power and 2.5 ms pulse duration.

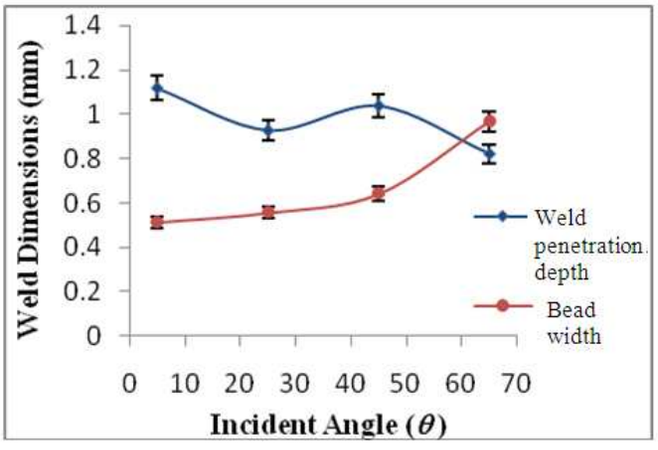

Figure 13. Characterictics of a spot weld dimensions when Nd:YAG laser spot incident angle is varied with respect to the stainless steel 304 surface normal by employing 2.5 kW laser peak power and 2.5 ms pulse duration.

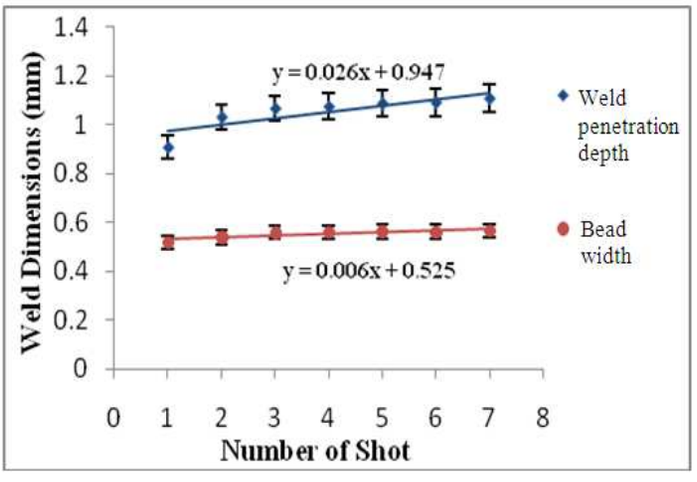

Figure 14. Spot weld produced by 2.5 kW laser peak power, 2.5 ms pulse duration with laser beam incidence is vertical in respect to the surface normal and laser focus point is on the stainless steel 304 surface, while the laser beam shot numbers are varied.

5. The strength analysis of a welding joint

In this section, the strength test of a welding joint of a single spot welding is discussed for stainless steel 304. A test is also executed for a seam welding which is produced by shooting the laser pulses continuously along the 10.0 ± 0.1 mm stainless steel 304 interfaces. The strength for seam welding of stainless steel 304 is also compared to an Invar™, which is a commercial welding material for photonics device packaging. A Unitek Miyachi LW10E ultra compact pulsed Nd:YAG laser with wavelength of 1.064 μm is employed to produce a weld joint. The energy per pulse output is in the range of 1 to 20 J, laser beam peak power is up to 3.5 kW and pulse duration ranging from 0.3 ms to 10.0 ms. However, in this investigation, only 3.5 kW laser beam peak power and 6.5 ms pulse duration is employed. This parameter is chosen because it produces a deepest penetration depth on stainless steel 304 which is 1.2 mm (Nawi et al., 2011). The penetration depth is important and should be large enough to achieve a strong attachment. The welding base material used is a stainless steel 304 sheet with a thickness of 1.0±0.1mm. The experimental setup to produce a weld consists of a laser source, fiber optics delivery system, and focusing lenses with focal length of 100.00 mm as illustrated in Figure 14.

The optical fiber cables transmit the laser beam to the welding focusing lenses inside the lens housing. The laser welding system is also equipped with an aiming diode laser beam, which simplifies positioning of the laser spot on the stainless steel sheet. A spot weld and a seam weld are produced with two types of joint; butt joint and lap joint, as illustrated in Figures 15(a) and 15(b). The strength of the weld joints is conducted by pulling the joint materials using INSTRON Series IX/s Automated Materials Tester System. The crosshead speed utilized for pulling the joint is set to 0.2 mm/min. The strength for a weld joint is determined by measuring the applied load during the test.

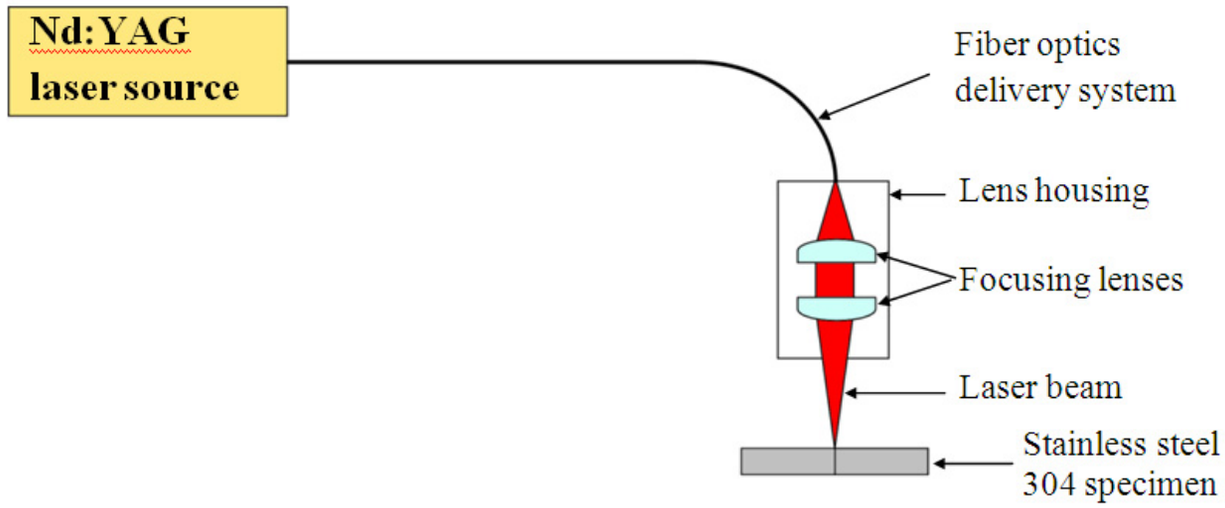

Figure 15. Nd:YAG laser experimental setup to produce a spot weld on stainless steel 304 specimen.

The element composition of stainless steel 304 and welded stainless steel 304 are examined by using Energy Dispersive X-ray (EDX) technique. The stainless steel 304 consists of iron (Fe) 69.59wt%, chromium (Cr) 18.33wt% and nickel (Ni) 12.08wt%. Figure 16 shows the element composition for stainless steel 304 changes when it is welded by Nd:YAG laser beam and it is now comprising of iron (Fe) 68.83wt%, chromium (Cr) 17.10wt% and nickel (Ni) 14.08wt%. It is observed that there are no changes in the elemental composition before and after welding of stainless steel 304. The applied load for the test and the pulling displacement for spot and seam welding are shown in Figure 17 and Figure 18, respectively. Maximum applied load is considered as the strength of the weld joint. Figure 16 illustrates maximum load for butt and lap joint which are 0.2296 kN and 0.0691 kN with a pulling displacement of 0.43 mm and 0.40 mm, respectively.

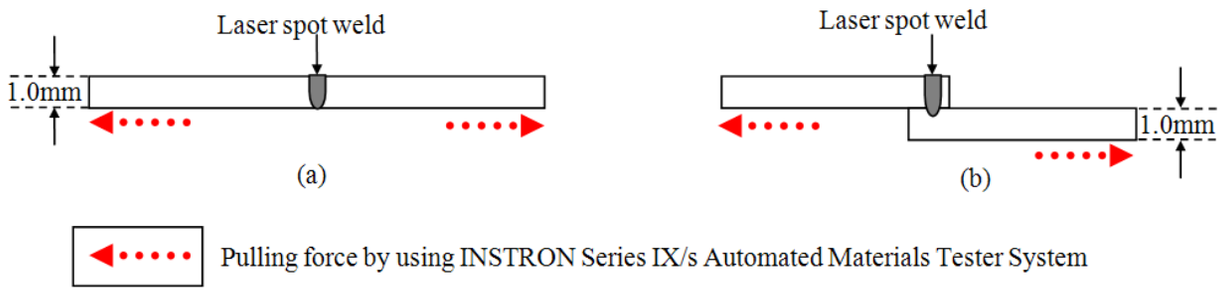

Figure 16. Configuration of the (a) butt joint and (b) lap joint, for stainless steel 304 with a thickness 1.0±0.1mm.

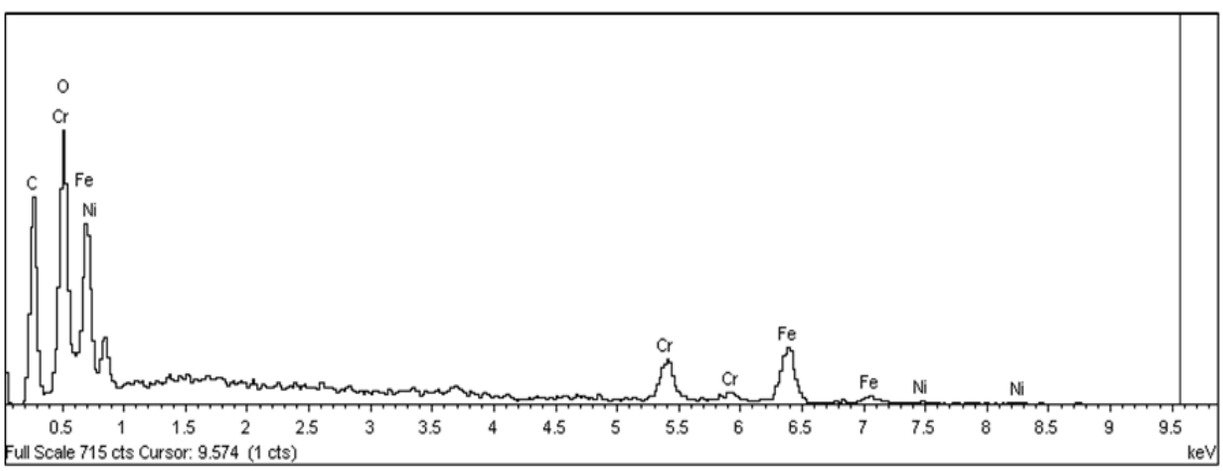

Figure 17. EDX analysis for the elemental composition of welded stainless steel 304.

The Invar™ maximum load is recorded as 0.3760 kN with 0.43 mm pulling displacement. The outcome indicates that the butt joint produces much stronger attachment than the lap joint. The stronger attachment is contributed by a larger volume of welded stainless steel at the joint interfaces as shown in Figure 19(a). For lap joint, the thickness of the stainless steel 304 becomes double as the upper and lower stainless steel sheets are overlapped. If

the laser beam produces insufficient penetration depth, thus only a small volume of welded stainless steel 304 is produced at the interfaces of the joint as shown in Figure 19(b). This will lead to a weaker joint. But, the penetration depth can be increased by controlling the laser beam parameters such as laser beam peak power and pulse duration. Hence, it will increase the strength of a lap joint. In terms of welding materials comparison, the commercial welding material, Invar™, provides more robust joint than stainless steel 304. Figure 18 indicates the seam welding maximum load for butt joint is 2.6339 kN with 0.62 mm pulling displacement. Lap joint recorded the maximum load of 1.0466 kN at 0.49 mm. This implies that the butt joint of a seam welding provides a much stronger attachment than the lap joint similar with the case of a single spot weld. Figure 18 also indicates between the butt joint pulling displacement of 0.48 mm and 0.72 mm, there are no significant changes in the joint strength because each point along the seam welding has the similar maximum strengths but it is not achieved simultaneously depending on its geometry.

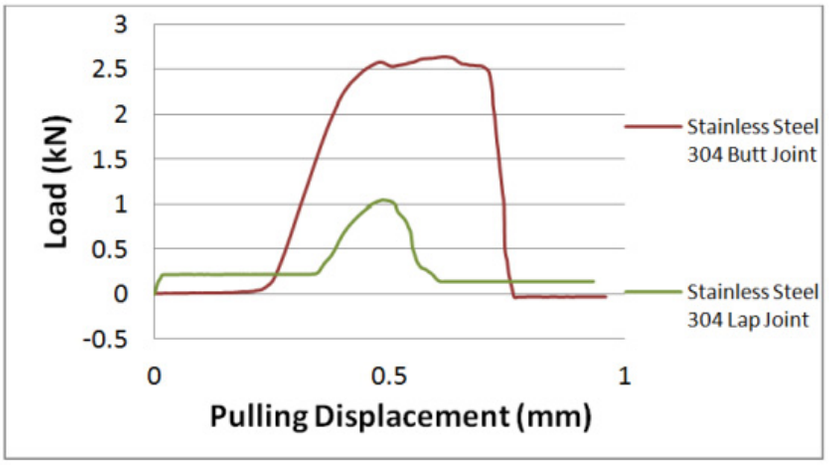

Figure 18. Strength profile of a single spot weld produced on stainless steel 304 and Invar™ by using 3.5 kW Nd:YAG laser beam peak power and 6.5 ms pulse duration.

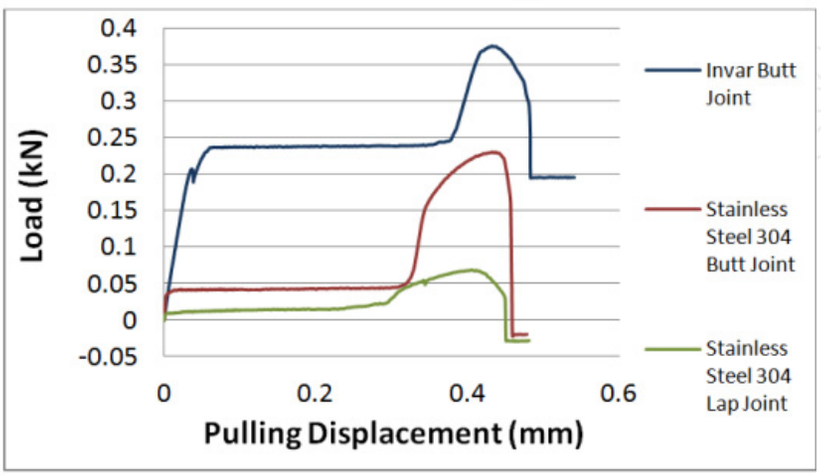

Figure 19. Strength profile of a seam weld produced on a stainless steel 304 along 10.0 ± 0.1 mm joint interfaces.

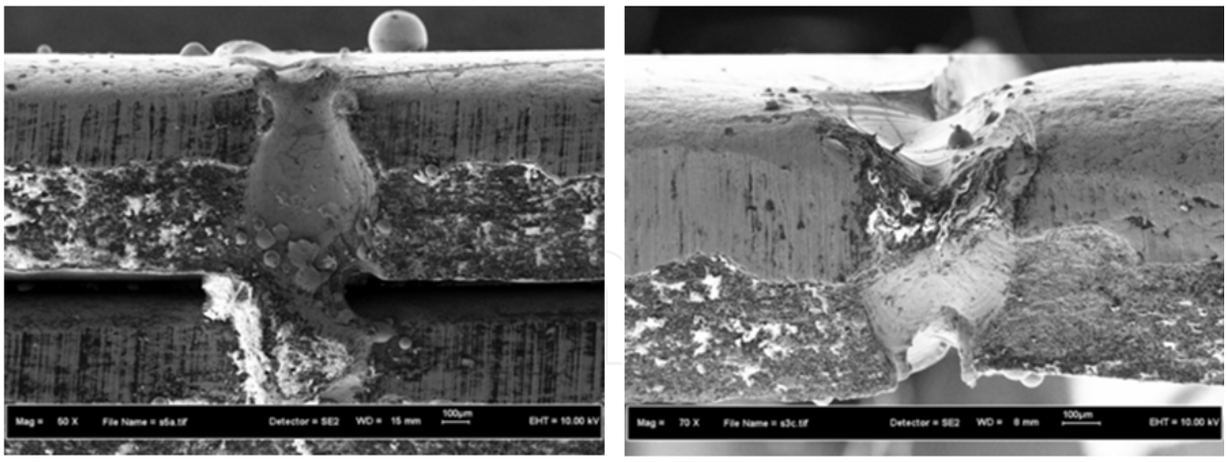

a) b)

Figure 20. FESEM micrographs of a stainless steel 304 spot weld joint; (a) butt joint and (b) lap joint, produced by 3.5 kW laser beam peak power and 6.5 ms laser pulse duration.

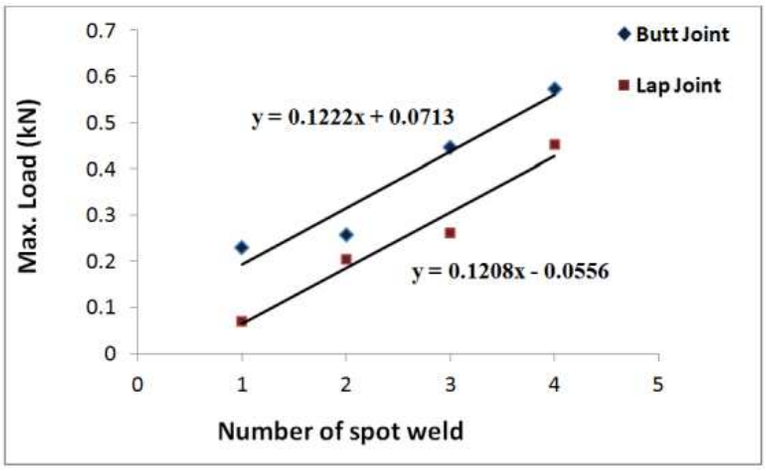

Figure 21. The strength comparison between butt joint and lap joint for variation number of spot weld.

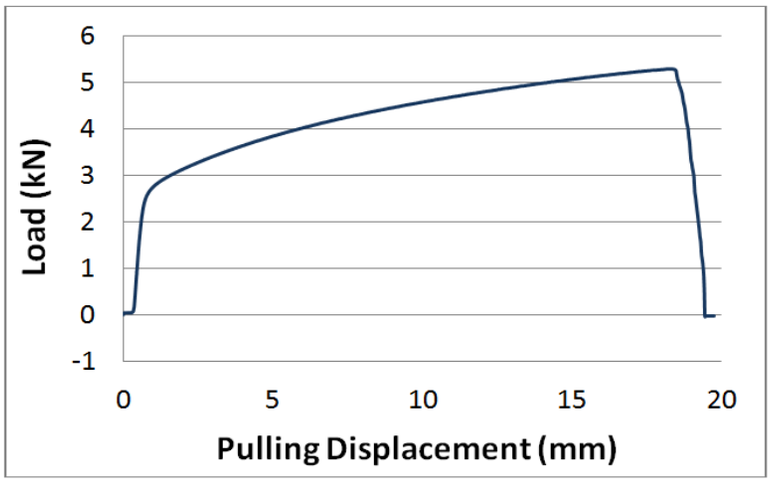

Figure 22. The strength of a stainless steel 304 with 1.0 ± 0.1 mm thickness and 10.0 ± 0.1 mm width.

In miniature assemblies, only a small number of laser spot weld is used for an attachment because of the relative small parts (Fadhali et al., 2007a, 2007b, 2007c, 2007d, 2008). The strength on the number of laser spot welding up to four spots is investigated for butt joint and lap joint. Then, the maximum strength for both joint types is compared. Figure 20 illustrates that the strength increases when the number of spots increases for butt and lap joint. A linear relationship is obtained from both joints strength against the number of spots and it has equal gradient which are 0.122 and 0.120, respectively. This suggests there is no significant difference in the influence of number of spots on the strength for both types of joint. The strength of stainless steel 304 is shown in Figure 21. It produces a strength of 5.2866 kN with 18.23 mm pulling displacement. The strength of stainless steel 304 is almost twice stronger than the seam welded stainless steel 304. Thus the welded material cannot attain the strength of the base material itself. The pulling displacement indicates that the elastic modulus of stainless steel 304 is much more greater than the welded stainless steel 304.

6. Conclusion

In conclusion, it is shown that the penetration depth and bead width increase when the laser beam peak power, pulse duration and number of shot are increased. It is found that the laser peak power is more effective to produce the deeper penetration depth rather than the bead width. Otherwise, the laser beam pulse duration is an accurate parameter to control if the desired bead width is required rather than the penetration depth. As the focus point positions are placed forward and backward from the stainless steel 304 specimen surface, the laser spot size increases. This leads to the reduction of the laser beam intensity. Hence, the penetration depth decreases. The increase of the laser spot size will increase the bead width. When the laser beam incident angle is varied, the bead width also changes due to the widening of the laser spot size. The penetration depth depends on the both widening laser spot size and material surface reflectivity that drops due to the influence of light polarization. The penetration depth increases slightly with the number of shots due to the material ablation produced by laser pulse pressure when it strikes the specimen surface. For welding joint strength, a butt joint produces much stronger attachment than a lap joint. The stronger attachment is contributed by a larger volume of welded stainless steel 304 at the joint interfaces. It is observed that each point along the seam welding has a similar maximum strengths but it is not achieved simultaneously. The similar gradient obtained in a linear relationship suggests that there is no significant difference in the influence of number of spots on the butt and lap joint strength. The commercial welding material, Invar™, provides more robust joint rather than stainless steel 304. The welded stainless steel 304 cannot attain the strength and elastic modulus of the stainless steel 304 itself. From the strength test results, it is found that stainless steel 304 is a good candidate to be used as a welding material for photonics device packaging by using pulsed Nd:YAG laser welding technique.

Author details

Ikhwan Naim Md Nawi
Centre of Foundation Studies & Faculty of Applied Sciences, Universiti Teknologi MARA, Malaysia

Jalil Ali
Universiti Teknologi, Malaysia

Mohamed Fadhali
Physics Department, Faculty of Science, Ibb University, Yemen

Preecha P. Yupapin
King Mongkut's Institute of Technology Ladkrabang, Bangkok, Thailand

7. References

Beretta, J.R.; Rossi, W.; Neves, M.D.M.; Almeida, L.A. & Vieira, N.D. (2007). Pulsed Nd:YAG laser welding of AISI 304 and 420 Stainless Steel. *Journal of Optical Lasers Engineering*, Vol. 45, pp. 960-966.

C. Dawes, C. (1992). *Laser welding: A practical guide*. Woodhead Publication Ltd., England.

Fadhali, M.; Zainal, J.; Munajat, Y.; Ali, J. & Rahman, R. (2007a). Reliable pigtailing of photonic devices employing laser microwelding. *Journal Engineering and Applied Science*, Vol. 2, pp. 1724-1728.

Fadhali, M.; Zainal, J.; Munajat, Y.; Ali, J. & Rahman, R. (2007b). Investigation of the application of Nd:YAG laser welding to couple photonic devices and packaging. *Lasers Engineering*, Vol. 17, pp. 273-286.

Fadhali, M.; Zainal, J.; Munajat, Y.; Ali, J. & Rahman, R. (2007c). Laser diode pigtailing and packaging using Nd:YAG laser welding technique. *Jurnal Komunikasi Fisika Indonesia*, Vol. 5, pp. 203-208.

Fadhali, M.; Zainal, J.; Munajat, Y.; Ali, J. & Rahman, R. (2007d). Analysis of laser microwelding applied for photonic devices packaging. Journal Solid State Science and Technology Letter, Vol. 14, pp. 18-19.

Fadhali, M. (2008). Efficient coupling and reliable packaging of photonic devices using laser welding technique. *Ph.D Thesis: Universiti Teknologi Malaysia*, Skudai, Johor, Malaysia.

Kazemi, K & Goldak, J.A. (2009). Numerical simulation of laser full penetration welding. *Computer Material Science*, Vol. 44, pp. 841–849.

Marley, C. (2002). Laser welding photonics devices: Proper design guidelines enable users to achieve high-precision alignment requirements. *Industrial Laser Solutions for Manufacturing*, 2002.

Mousavi, S.A.A. & Sufizadeh, A.R. (2008). Metallurgical investigations of pulsed Nd:YAG laser welding of AISI 321 and AISI 630 stainless steels. *Journal of Material Design*, Vol. 15, pp. 44-49.

Naim, I.; Saktioto, T.; Fadhali, M.; Ali, J.; & Yupapin, P.P. (2009). An investigation of a pulsed Nd:YAG laser welding technique. *Proceedings of IEEE-Regional Symposium on Micro and Nanoelectronics*, pp. 274-280, Kelantan, Malaysia, August 10-12, 2009.

Naim, I.; Saktioto, T.; Hamdi, M.; Fadhali, M.; Ali, J.; & Yupapin, P.P. (2010). Penetration depth estimation for stainless steel 304L using Nd:YAG laser spot micro welding. Proceedings of 2nd Topical Meeting on Lasers and Optoelectronics, Vol. 1, pp. 278-288, Terengganu, Malaysia, March 13-15, 2010.

Nawi, I.N.; Saktioto; Fadhali, M.; Hussain, M.S.; Ali, J. & Yupapin, P.P. (2011). A Reliable Nd:YAG Laser Welded Stainless Steel 304 for Photonics Device Packaging. *Procedia Engineering*, Vol. 8, pp. 380-385.

Pang, M.; Yu.G.; Wang, H.H. & Zheng, C.Y. (2008). Microstructure study of laser welding cast nickel-based superalloy K418. *Journal of Material Processing Technology*, Vol. 207, pp. 271–275.

Ready, J.F. (1997). *Industrial applications of lasers*. New York: Academic Press.

Zhou, J. & Tsai, H.L. (2008). Modeling transport phenomena in hybrid laser-MIG keyhole welding. *Internattonal Journal of Heat and Mass Transfer*, Vol. 51, pp. 4353-4366.